OPEN ACCESS

Original research

Parent artery-initiated and stent-mediated neointima formation in a rat saccular side wall model

Stefan Wanderer ,[1,2] Basil Erwin Grüter ,[1,2] Gwendoline Boillat,[1,2] Sivani Sivanrupan,[2] Jeannine Rey,[1,2] Kristina Catalano,[2] Michael vonGunten,[3] Hans Rudolf Widmer,[4] Lukas Andereggen,[1,2] Serge Marbacher [1,2]

► Additional supplemental material is published online only. To view, please visit the journal online (http://dx.doi.org/10.1136/neurintsurg-2021-018297).

[1]Neurosurgery, Kantonsspital Aarau AG, Aarau, Switzerland
[2]Cerebrovascular Research Group, Department for BioMedical Research, University of Bern, Bern, Switzerland
[3]Institute of Pathology Laenggasse, Ittigen, Switzerland
[4]Neurosurgery, Inselspital Universitatsspital Bern, Bern, Switzerland

Correspondence to
Dr Stefan Wanderer, Neurosurgery, Kantonsspital Aarau AG, Aarau, Switzerland; stefan_wanderer86@gmx.de

SW and BEG contributed equally.

SW and BEG are joint first authors.

Received 5 October 2021
Accepted 29 November 2021

To cite: Wanderer S, Grüter BE, Boillat G, *et al*. *J NeuroIntervent Surg* Epub ahead of print: [*please include* Day Month Year]. doi:10.1136/neurintsurg-2021-018297

ABSTRACT

Background Unlike clipping that forms an immediate barrier of blood flow into intracranial aneurysms, endovascular treatments rely on thrombus organization and neointima formation. Therefore, a continuous endothelial cell layer is crucial to prevent blood flow in the former aneurysm. This study investigates the origin of endothelial cells in the neointima of endovascular treated aneurysms, specifically whether cells from the parent artery play a role in neointima formation.

Methods In male rats, decellularized and vital side wall aneurysms were treated by coil (n=16) or stent embolization (n=15). The cell tracer CM-DiI dye was injected into the clamped aorta before aneurysm suture to mark initial endothelial cells in the parent artery and enable tracking of their proliferation during follow-up. Aneurysms were analyzed for growth, thrombus formation, and recurrence. Histological evaluation followed with cell counts for specific regions-of-interest.

Results During follow-up, none of the 31 aneurysms ruptured. Macroscopic residual perfusion was observed in 12/16 rats after coiling and in 1/15 after stenting. Amounts of CM-DiI +cells in coiled versus stented decellularized aneurysms significantly decreased in the thrombus on day 7 (p=0.01) and neointima on day 21 (p=0.04). For vital aneurysms, the number of CM-DiI +cells in the neointima on day 21 showed no significant difference.

Conclusions Healing patterns were worse in coil-treated than stent-treated aneurysms. Cell migration forming a neointima seemed mainly dependent on the adjacent vessel in decellularized aneurysms, but appeared buoyed by recruitment from aneurysm wall cells in vital aneurysms. Therefore, a cell-rich parent artery might be crucial.

INTRODUCTION

During the past decades, endovascular treatment has gained increasing importance in the management of both ruptured and unruptured intracranial aneurysms. Nevertheless, recurrence rates after coil embolization remain notably high compared with clip ligation.[1–4] Unlike direct mechanical occlusion of an aneurysm sac by clipping, an endovascularly treated patient awaits a biological healing response of thrombus organization and neointima formation as mediated by cell migration.

Smooth muscle cells (SMCs) play an important role in inducing aneurysm healing on a biological level. Preclinical and clinical studies have revealed that loss of mural cells predisposes aneurysm growth and rupture,[5–7] and that healing after coil embolization is worse in aneurysms with highly degenerated walls than in those with SMC-rich walls.[8] Cell-based therapies with intraluminal transplantation of SMCs were shown to promote complete aneurysm healing along with prevention of growth and rupture.[9] In a comparison of endovascular devices, better aneurysm healing was demonstrated in stented compared with coiled aneurysms[10]; likewise neointima formation and thrombus organization are concurrent processes in aneurysm healing, that depend on cell migration from both the parent artery and aneurysm wall. Neointima formation relied more on cell migration from the aneurysm wall in coiled aneurysms, whereas the role of cells originating from the parent artery seemed to be higher in stent-treated aneurysms.[11] These factors suggest that cell migration, allowing for a continuous endothelial lining along the parent artery's lumen, substantially contributes to complete aneurysm healing after endovascular treatment.

Until now, the origin of cells (aneurysm wall, parent artery or progenitor cells) responsible for aneurysm healing has remained unclear.[12 13] Whether the endothelial lining is triggered by progenitor cells, which have already been identified as attaching in stented animal aneurysm models,[14] or the parent artery itself has not yet been adequately analyzed. Toward this aim, our experimental study in a rat saccular side wall aneurysm model examined the origin of neointima-forming cells. Using a cell tracer injection, we analyzed the role of endothelial cells originating in the parent artery in neointima formation.

MATERIAL AND METHODS

Animals

After randomly assigning 12-week-old male Lewis rats (n=31; mean weight 498±8 g at baseline, 491±8 g at follow-up) to one of the four experimental groups, all underwent coiling or stenting treatment by using the Helsinki saccular side wall model within 6 weeks.[6] The rats were housed in groups of four animals at a room temperature accompanied by a 12 hour light/dark cycle. Free access to pellet and water was provided and care was in accordance with the local institutional guidelines. Animal experiments were approved by the Local Committee for Animal Care of the Canton

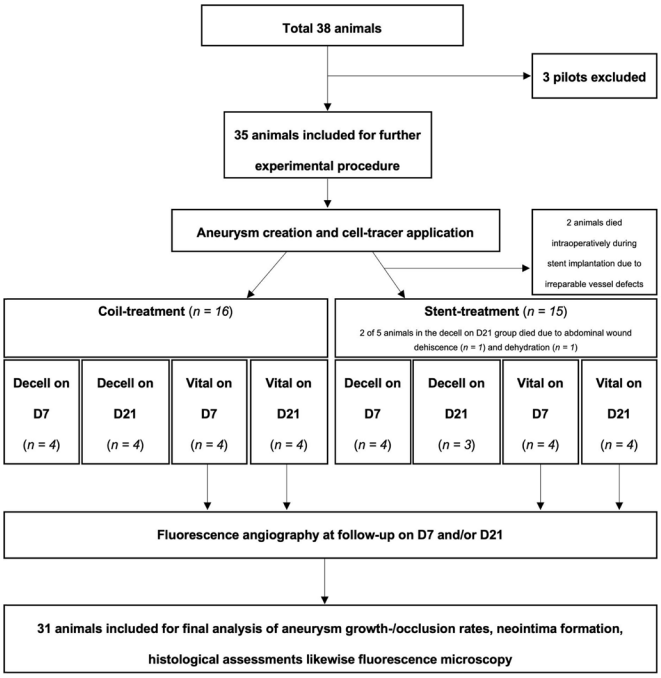

Figure 1 Flowchart of the study design. Of a total of 38 rats, 31 were included for final analysis and seven were excluded (three in the pilot study and four early dropouts).

Bern, Switzerland (BE 108/16; BE 60/19). For all experimental procedures the ARRIVE (Animals in Research: Reporting of In Vivo Experiments) guidelines were strictly followed.[15] Animal caregivers were blinded to all therapeutic steps and outcomes.

Study design

The study setting consisted of four groups that included (1) decellularized coiled, (2) vital coiled, (3) decellularized stented, and (4) vital stented aneurysms. Techniques have been described elsewhere for the coil device (2 cm of Target 360 TM Ultra, 2 mm diameter; Stryker, Kalamazoo, MI) and stent device (modified magmaris device, AMS with polymer coating, 6 mm length, 2 mm diameter, square-shaped struts 150 µm in thickness and 150 µm in width; nominal pressure of 8 bar; Biotronik, Bülach, Switzerland).[8 10 16] Side wall aneurysms were created by end-to-side anastomosis of a previously ligated arterial vessel pouch from the thoracic part of a donor animal. Each saccular pouch was sutured onto the clamped abdominal aorta of the recipient directly followed by either coil or stent implantation.[5]

Arterial pouches for decellularization were incubated in 0.1% sodium dodecyl sulfate for 10 hours at 37°C as previously described.[11] Vital aneurysm pouches were characterized as cell-rich aneurysm pouches. Coil and stent groups were designated as decellularized or vital at follow-up evaluation on days 7 and 21.

Before surgery, randomization to either the coil or stent treatment was performed using a web-based randomization system (www.sealedenvelope.com) (figure 1). Of the 38 rats operated on, 31 animals underwent coil (n=16) or stent (n=15) treatments and seven animals were excluded (three in the pilot study, four early dropouts). After euthanasia, the aneurysm and its parent artery were harvested for further histological processing.

Primary endpoints were defined as the proportion (%) CM-Dil +cells tracked for one of the following regions of interest: (1) aneurysm wall, (2) intraluminal thrombus, (3) neointima, and (4) parent artery. Secondary endpoints analyzed were aneurysm healing (by macroscopic and fluorescence examination) and histological analysis as defined by neointima formation, aneurysm wall cellularity and inflammation, periadventitial inflammation, and fibrosis.

Anesthesia protocol

For initial induction of anesthesia, all rats were placed in a clean box with oxygen (O_2) provided until the animal lost consciousness (5–10 min). Next, rats were anesthetized with a subcutaneous injection of a mixture of fentanyl 0.005 mg/kg (Sintetica, S.A. Switzerland), medetomidine 0.15 mg/kg (Virbac, Switzerland), and midazolam 2 mg/kg (Roche, Switzerland). This protocol ensured a surgical plane of at least 45 min. In cases requiring prolonged anesthesia, isoflurane was started (1.0–2.0% titrated to effect in 100% O_2 administered via face mask) to allow adequate surgical anesthetic depth and analgesic coverage throughout (detailed anesthesiological protocol given in online supplemental methods).

Cell tracer injection

The fluorescent lipophilic CellTracker CM-Dil dye (Invitrogen, Molecular Probes, MW 1051.50; Eugene, OR) was stored light-protected at ≤ −20°C at all times (pretesting of the functionality is described in online supplemental figure 1). On the day of the experiment, CM-Dil dye (2 µL was dissolved in 1 mL phosphate-buffered saline and transferred to a 1 mL syringe with a 27-1/2 gauge (0.4×13 mm) cannula; both steps were taken under light protection. Lights in the operating room were turned off. After clamping the proximal and distal parts of the abdominal aorta, the corresponding vessel segment was flushed with heparinized 0.9% saline solution and the CM-Dil dye was carefully injected. Immediately, the microscope light was also turned off. After a 15 min incubation period, room lights and the microscope light were turned on and the longitudinal arteriotomy and suturing of the aneurysm proceeded.

Likewise, three pilots were created with cell tracer injection. Next, decellularized aneurysms were sutured end-to-side on the aorta. With euthanasia of the animals immediately after labeling, the dye appeared uniformly distributed and the proportions of CM-Dil dye +cells were 100% in the vessel wall (online supplemental figure 2).

Patency evaluation, macroscopic inspection and soft tissue preparation

Fluorescence angiography was performed to assess dynamic perfusion status of the aneurysm after intravenous injection of 2 mL fluorescein (fluorescein 10% Faure, 0.5 g/5 mL), followed by illumination (light source 465–490 nm) that was filmed with a specific detection filter as previously described.[17 18] After the animals were euthanized with an overdose of intracardial ketamine hydrochloride (Narketan, 120 mg/kg ketamine injection, Vetoquinol, Switzerland), the aneurysms were harvested and measured in three dimensions (length, width, height). The posterior aorta was opened to inspect the aneurysm orifice in coiled animals. Tissues were immediately fixed in formalin (4% weight/volume solution, J.T. Baker, Arnhem, The Netherlands) until paraffin embedding for histological analysis was performed.

Measurement of the pre- and post-mortem aneurysm volume, histology

The aneurysm was documented before implantation and at harvesting using a digital camera (Sony NEX-5R, Sony, Tokyo, Japan) attached to a microscope (OPMI, Carl Zeiss AG, Oberkochen, Germany). Aneurysm volume was calculated with the

cylindric formula: $\pi \times$ height $\times$ width/2 $\times$ length/2 (online supplemental table 1).

Post-mortem, under the microscope, coils were carefully retrieved with micro instruments. Further histological processing was proceeded with stents in situ. Paraffin-embedded aneurysms were cut along the axis of the corresponding parent artery, in 2 µm sections, and stained; stains included hematoxylin and eosin (H&E), smooth muscle actin (SMA), Masson-Goldner trichrome (MASA), and Von Willebrand factor (F8). After digitalization of slides followed by Omnyx (VL 120, GE), each slide was evaluated using the JVS viewer (JVS view 1.2 full version, http://jvsmicroscope.uta.fi/software/, University of Tampere, Finland). All light microscopy samples underwent blinded qualitative analysis by two independent observers (SW and BEG) and were rated with a previously used four-tier grading system.[5] Periadventitial inflammation, aneurysm wall inflammation, number of neutrophils in the thrombus, and aneurysm wall cellularity were analyzed in H&E stained, periadventitial fibrosis, and neointima formation in MASA-stained slices. Furthermore, the number of endothelial cells in the thrombus was analyzed, specifically regarding the potential role of endothelial clefts as the main reason for aneurysm recurrence.

For fluorescence microscopy, slides were cut to a 4 µm thickness, deparaffined, and stained by DAPI (4',6-diamidino-2-phenylindole) application. CM-Dil dye staining had been completed intraoperatively in vivo. Slides were photographed digitally using a fluorescence microscope (Olympus BX51, Hamburg, Germany; Cell Sens Dimension Imaging software v1.8) with exposure times of 50 ms for DAPI and 90–130 ms for TXRED. The proportions of CM-Dil dye +cells on all cells were calculated using a semi-automated, cell count software (Image-J version 1.52 n, US National Institutes of Health, Bethesda, MD, https://imagej.nih.gov/ij/) for four regions of interest: (1) aneurysm wall, (2) inside thrombus and (3) neointima, and (4) parent artery. For cell counting, a size from 7 to 100 (infinity) and a circularity for corresponding analyzed particles from 0.3 to 1.00 was applied.

Exclusion criteria and statistical analysis

Exclusion from final analysis were premature death or euthanasia for any reason. Statistical analyses were performed using the non-parametric Wilcoxon-Mann-Whitney-U test. A probability value of $p<0.05$ (*) and $p<0.01$ (**) was considered significant. Data were analyzed by IBM SPSS (version 22, USA) and visualized by Graph Pad Prism 8 (Version 8.2.0.435, GraphPad software, San Diego, CA). Sample size per group was determined using a priori sample size calculation (BiAS.for.Windows Version 11, epsilon Verlag, Germany). To achieve $\alpha=0.05$ at $\beta=0.2$ with a sigma (σ) of 0.2, the sample size calculation showed that n=4 animals per group were appropriate to achieve a delta (δ) between 0.3 and 0.5. All values given in the text are expressed as mean±SD or median and IQR.

RESULTS

In decellularized aneurysms, the amounts of CM-Dil +cells in the neointima did not significantly differ between stent-treated or coil-treated animals at 7 days ($p=0.77$), but were significantly higher in stent-treated animals at 21 days ($p=0.04$) (figure 2A). For vital aneurysms, no significant differences were noted at either 7 days ($p=1.0$) or 21 days ($p=0.66$) (figure 2B). A pooled-analysis comparing decellularized coiled versus stented aneurysms showed no significant differences regarding neointima formation ($p=0.38$), cells in the aneurysm wall ($p=0.81$), or periadventitia ($p=0.35$). Significant differences of CM-Dil dye +cells were found for thrombus invasion in the stent group ($p=0.017$). A pooled-analysis comparing vital coiled and stented aneurysms showed no overall significant differences in neointima ($p=0.87$), thrombus ($p=0.83$), aneurysm wall ($p=0.74$), and parent artery ($p=0.26$).

Overall, four of 35 animals died, yielding an 11.4% mortality rate. The four deaths included two animals with irreparable vessel defect suffered intraoperatively during stent implantation, and two animals in the decellularized stenting group whose euthanasia was planned for day 21 (one for abdominal wound dehiscence, and one for dehydration due to inadequate food and water intake).

Aneurysm growth after treatment

Baseline aneurysm volumes did not statistically differ between coiling and stenting, respectively, in the decellularized group (17.15±6.40 mm^3 vs. 14.60±3.50 mm^3; $p=0.86$) or vital group (17.10±3.01 mm^3 vs. 11.87±5.87 mm^3; $p=0.10$) (online supplemental figure 3); aneurysm volumes depicted were pooled (ie, combined follow-up days 7 and 21) as a single value. In follow-up comparisons, decellularized aneurysms showed a non-significant tendency toward more pronounced aneurysm growth in the coiled group than stented group (38.15±23.47

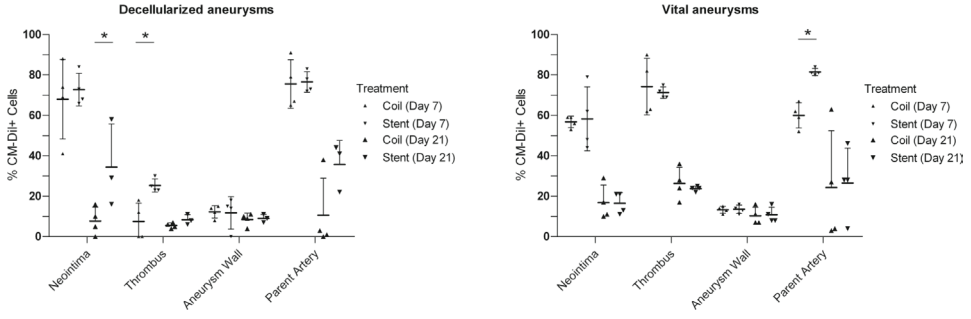

Figure 2 Left panel shows cell count comparison between different regions of interest (ROI) in coil- and stent-treated decellularized aneurysms. Graph depicts the cumulative relative cell counts for CM-Dil +cells in decellularized aneurysms sutured on the abdominal part of the aorta, either coil- or stent-treated. Treatments were compared for coiled and stented groups in decellularized aneurysms on days 7 and 21. Significant differences in the proportion of CM-Dil +cells in the neointima for day 21 and thrombus for day 7 ($p<0.05$) were observed. Right panel shows cell count comparison between different ROIs in coil- and stent-treated vital aneurysms. Graph depicts the cumulative relative cell counts for CM-Dil +cells in vital aneurysms sutured on the abdominal part of the aorta, either coil- or stent-treated. Treatments were compared for coiled and stented groups in vital aneurysms on days 7 and 21. Significant differences in the proportion of CM-Dil +cells in the parent artery for day 7 ($p<0.05$) were observed.

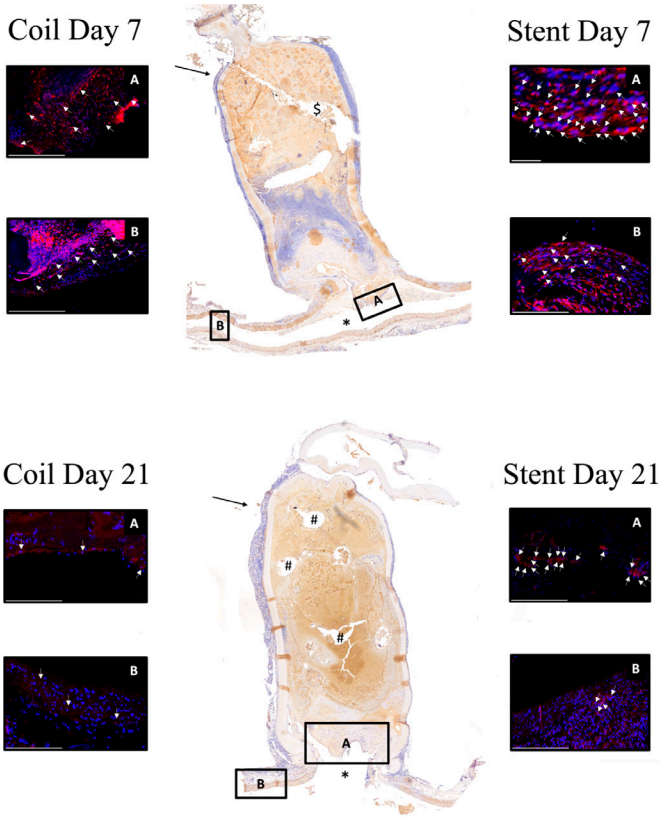

Figure 3 Illustrative panel of CM-Dil +cell distribution in a decellularized aneurysm with coil- and stent-treatment postoperatively. Panel A, coil day 7/stent day 7. Left-side depicts a coil-treated aneurysm, immunostaining for neointima (A) and parent artery (B) performed. Right side shows same setting performed for stenting 7 days postoperatively. CM-Dil +cells are found in the neointima more pronounced for stent-treatment (scale bar 100 µm left, 200 µm right). Middle, image overview of monoclonal anti-α muscle actin (a-SMA) positive cells (twofold magnification) with stent-treatment 7 days postoperatively; $ shows fixation artifact. In panel B (coil day 21/ stent day 21), immunostaining for neointima (A) and parent artery (B) demonstrates decreased CM-Dil +cells in coil-treated compared with stent-treated aneurysms (p<0.05). (A) Magnified area of the neointima. CM-Dil +cells are found in the neointima (scale bar 100 µm left, 100 µm right). (B) As well, CM-Dil uptake is registrated in the parent artery. Middle, image overview of monoclonal anti-α muscle actin (a-SMA) positive cells in an aneurysm with a twofold magnification after coil treatment 21 days postoperatively is shown. *Lumen of the parent artery; #coil artifact.

mm^3 vs. 22.42±7.92 mm^3; *p=0.28)*. At follow-up, this growth was significantly greater in the vital group for coiled versus stent-treated aneurysms (60.10±31.12 mm^3 vs. 20.51±20.65 mm^3; *p=0.002*) (online supplemental figure 3). At follow up, fluorescence angiography indicated reperfusion in 6/6 (100%) coiled animals and in 1/8 (12.5%) with stent treatment (online supplemental figure 4). Evolution of aneurysm healing is depicted by time in online supplemental figure 5.

Microscopic healing status

All aneurysms demonstrated progressive healing patterns with increased neointima thickness and advanced thrombus organization (detailed histological analysis of all aneurysms in online supplemental figure 6; aneurysm volumes are depicted pooled).

Periadventitial inflammation was significantly reduced in the decellularized coil group compared with the decellularized stent group (p=0.003); no effects were observed between vital-coiled and vital-stented aneurysms (p=0.36). Periadventitial fibrosis was significantly reduced in the decellularized coil group compared with the decellularized stent group (p=0.0006) and vital counterparts (p=0.014). Aneurysm wall inflammation was significantly reduced in the decellularized coil group compared with the decellularized stent group (p=0.0046). Neointima formation was significantly enhanced in the decellularized stent group compared with the decellularized coil group (p=0.036), and in the vital group in favor to stent treatment (p=0.0012).

Fluorescence analysis for neointima, thrombus, aneurysm wall and parent artery

In decellularized aneurysms, the amount of CM-Dil +cells in the neointima did not differ between stent-treated and coil-treated animals at 7 days (p=0.77), but was significantly higher in stent-treated animals at 21 days (p=0.04) (figures 2 and 3). For vital aneurysms, no significant differences were noted between groups at 7 days (p=1.0) or 21 days (p=0.66) (figure 2). In decellularized aneurysms, after 7 days significantly more CM-Dil +cells were found in the thrombus of the stented-treated group (p=0.01).

For vital aneurysms, a significant enhancement in CM-Dil +cells was observed in the parent artery of stented animals on day 7 (p=0.02). In a pooled analysis, decellularized aneurysms showed significance in CM-Dil +cells in the thrombus for the stent group (p=0.017), whereas no differences were observed in the vital group for either coil or stent treatment. Proportions of CM-Dil +cells for all aneurysms are depicted in online supplemental table 2.

Surgical characteristics

Comparisons of surgical characteristics between coil- and stent-treated animals are depicted in online supplemental figure 7. Significant differences were found between coil and stent treatments, respectively, for operative time (119.06±21.35 min vs 154.13±30.20 min; p=0.001), the number of stitches to suture the aneurysm (15.62±2.87 vs 11.26±1.09; p=0.000002), and the total number of stitches (including further stitches performed when anastomosis was leaking) used for aneurysm suturing (15.93±2.86 vs 11.40±1.05; p=0.000002).

Physiological parameters

Vital signs monitored for the duration of the operation are depicted in online supplemental figure 8. In addition to pulse distension, we also analyzed breath distension, heart rate, oxygen saturation, breath rate, and temperature. Although breath distension was significantly reduced in stent-treated (12.95±0.71) versus coil-treated (13.51±0.63) rats (p=0.027), the other physiological variables did not show any significant differences.

DISCUSSION

In comparing healing of decellularized and vital aneurysms after coil and stent treatments, we demonstrated that neointima formation was mediated by endothelial cells originating in the adjacent parent artery in decellularized aneurysms whereas this lining was supported by cells derived from the aneurysm wall in vital aneurysms. This finding was consistent in short-term and intermediate follow-up. In turn, previous studies have already shown that the amount of circulating progenitor cells contribute only a minor role in aneurysm healing.[19 20]

A growing body of literature suggests that the various treatment options for intracranial aneurysms are not only efficacious but can be associated with the biological response of the wall itself.[5 7 9 11 12] Specifically, ligation provides an immediate direct endothelial contact whereas endovascular therapies rely more on biological processes, particularly the newly developed minimally invasive techniques, such as stent-assisted coiling, flow-diversion, web-device management, bioactive endovascular devices, systemic drug therapies or cell-based therapies.[9 10]

Previous studies have shown that neointima formation and thrombus organization are concurrent processes in aneurysm healing after endovascular therapies: both rely on cell migration from the parent artery and aneurysm wall, and both are facilitated by the presence of endovascular devices. Thrombus-organizing cells typically originate from the parent artery for both types of endovascular treatment, whereas neointima formation in coiled aneurysms relies more on cell migration from the aneurysm wall, in stent-treated aneurysms mostly from the parent artery.[11] In our experimental study, the parent artery was identified as an important source of migrating cells that form the neointima. This process happened in both forms of endovascular treatment and was observed within a few days from onset of aneurysm healing. During subsequent weeks, fading of the CM-Dil dye indicates the loss of signal intensity as these cells continue to divide at their new location, predominantly in the neointima and thrombus. The intensity of the lipophilic cell tracer decreases with each mitosis. These findings confirm the important role of endovascularly applied stents in a cell-rich region that serves as a principal structure for cell migration, which allows continuous endothelial lining, neointima formation, and progressive aneurysm healing.

In decellularized aneurysms, the number of CM-Dil +cells after stent versus coil treatments were higher on day 7 (72.25% vs 68%, p=0.77) and significantly higher on day 21 in the neointima (34.44% vs 7.75%, p=0.04). This finding suggests that cells involved in the aneurysm healing process migrated from the parent artery rather than the aneurysm wall. More importantly, we believe that the significantly greater number of CM-Dil +cells found in the thrombus after 7 days could be because the stent struts facilitated intraluminal thrombus formation in the aneurysm sac, which also seems explainable because the neointima is not sealed after 7 days. For vital aneurysms after coiling and stenting for days 7 (56.75% vs 58.25%, p=1) and 21 (11.5% vs 16.5%, p=0.66), no significant differences were found regarding CM-Dil +cells in the neointima; this finding supports the hypothesis that healing mechanisms in the coiled animals are stronger because of recruiting cells from the aneurysm wall (for endothelial staining via F8 please see online supplemental figure 9). In vital aneurysms, comparison of the number of CM-Dil +cells in coil versus stent treatments showed similar distributions in the aneurysm wall on day 7 (13.25% vs 13.5%, p=0.88) and day 21 (10.25% vs 10.75%, p=0.55); were similar for intraluminal thrombus formation on day 7 (62% vs 71.25%, p=1) and day 21 (26.25 % vs 23.75 %, p=0.55); and decreased in the parent artery on day 7 (60.0% vs 81.5%, p=0.02) and day 21 (24.25% vs 26.5%, p=0.46). The significantly higher amount of CM-Dil +cells in the parent artery of stented aneurysms might be because stent insertion causes more local reactions than coils and that neointima formation was initiated via stents overlapping the parent artery. Therefore, endovascular treatment via stent treatment might be crucial for highly degenerated aneurysm walls whereas coiling or stent-assisted coiling might be predominantly useful for aneurysms with relatively healthy vessel walls.

Interestingly, the proportion of CM-Dil +cells in the parent artery was higher at both day 7 and day 21 in the decellularized stent-treated group (76.6% vs 35.66% day) than in the coil-treated group (75.5% vs 10.5%). P values for both time-points, comparing the amount of CM-Dil +cells in the parent artery in the decellularized coil versus stented group on day 7, were non-significantly altered (p=0.77), and also when compared with 21 days (p=0.07). At 21-day follow-up, variations in levels of CM-Dil +cells of <10% in five rats might be explained by the natural course of the fading dye or longer operating times that potentially degraded the light sensitive dye.

On days 7 and 21, respectively, more CM-Dil +cells were detected inside the thrombus of the stent-treated group (25.25% vs 8.33%) than the coiled group (7.5% vs 5.5%). This might be reasonable because after 21 days the neointima is completely sealed in nearly all of the cases. CM-Dil +cell migration into the thrombus was significantly enhanced for stent treatments on day 7 (p=0.01), possibly facilitated by the strut-like stents themselves; after 21 days, the p value was not significantly altered (p=0.1). CM-Dil +cells in the aneurysm wall showed no differences between coil or stent treatments on day 7 (12.25% vs 11.75%, p=0.55) and day 21 (8.5% vs 9%, p=1). Regarding endothelial thrombus invasion, Raymond *et al* elucidated the role of stents in lowering aneurysm recanalization rate and decreasing recurrences after embolization in a side-wall aneurysm model with venous pouches.[21] In our experiments, the amounts and extent of invasion of endothelial cells into the thrombus was higher in the coil-treated than stent-treated groups; this finding corresponded with a higher aneurysm reperfusion rate in the coiled group.

In summary, cell migration, allowing for a continuous endothelial lining via stents along the cell-rich parent artery's lumen, may be the substantial prerequisite for complete aneurysm healing after endovascular therapy, and may be especially critical in highly degenerated aneurysms. The implication is that coiling in ruptured cerebral aneurysms might suffice to promote healing in patients with relative healthy vessel walls, but is likely insufficient in aneurysms with degenerated walls. In terms of clinical translation and future perspectives, our results align with a preliminary report in a preclinical series by Nevzati *et al*.[8] Coating endovascular devices, such as coils, with chemoattractants might be a therapeutic strategy to stimulate adjacent cells in a healthy parent artery to divide and migrate into the aneurysm thrombus.

Study limitations

Recent findings by Morel *et al*[22] showed the influence of sex hormones on aneurysm growth, intraluminal thrombus resolution, and wall inflammation in the same aneurysm model used for our experiments. Therefore, to avoid the confounding effect of estrogen or androgen or both hormones, we included only male rats. Moreover, we used a specific cell tracer for labeling the parent artery in an effort to differentiate which cells were derived from circulating cells in the blood stream and which were derived from true migration of neighboring cells. Although previous studies found strong signal intensity of myofibroblasts at days 7 and 21, we cannot exclude a slightly diminished signal intensity in endothelial cells that was related to time and cell division.[9] Lastly, our model used hemodynamic characteristics and subsequent biological processes, such as the rate of spontaneous thrombosis or aneurysm healing, which are relevantly influenced by the side wall constellation of the aneurysm.[23]

CONCLUSION

Our study in a rat side wall model corroborates previous findings that biological healing of endovascularly treated aneurysms depends on cell migration from the adjacent vessel and is additionally supported by recruitment of cells from the aneurysm wall in vital (cell-rich) aneurysms. However, in decellularized aneurysms, the adjacent vessel segment is the most important source of cells to promote healing. Therefore, cell migration is facilitated by use of endovascular devices, such as stents, that connect adjacent cell-rich tissues to the aneurysm orifice. In consequence, scaffolds should be placed in cell-rich healthy vessel regions, particularly for treatment of highly degenerated aneurysms. Vice versa, the success of these treatment strategies may depend on the presence of a healthy (cell-rich) endothelium in the adjacent vessel. Coil treatment alone might be sufficient for aneurysms with relatively healthy vessel walls.

Contributors Dr Wanderer (SW) and Dr Grüter contributed equally and share first authorship.

Funding This work was supported by the Swiss national science foundation (310030_182450) and the Centre for Vascular Intervention, Bülach, Switzerland.

Competing interests None declared.

Patient consent for publication Not applicable.

Ethics approval This study does not involve human participants.

Provenance and peer review Not commissioned; externally peer reviewed.

Data availability statement All data relevant to the study are included in the article or uploaded as supplementary information. NA.

ORCID iDs
Stefan Wanderer http://orcid.org/0000-0002-4510-5741
Basil Erwin Grüter http://orcid.org/0000-0002-6314-2482
Serge Marbacher http://orcid.org/0000-0001-6305-7571

REFERENCES

1 Yu L-B, Fang Z-J, Yang X-J, *et al*. Management of residual and recurrent aneurysms after clipping or coiling: clinical characteristics, treatments, and follow-up outcomes. *World Neurosurg* 2019;122:e838–46.
2 Zhang Y, Zhou Y, Yang P, *et al*. Comparison of the flow diverter and stent-assisted coiling in large and giant aneurysms: safety and efficacy based on a propensity score-matched analysis. *Eur Radiol* 2016;26:2369–77.
3 Zuo Q, Yang P, Lv N. Safety of coiling with stent placement for the treatment of ruptured wide-necked intracranial aneurysms: a contemporary cohort study in a high-volume center after improvement of skills and strategy. *J Neurosurg* 2018:1–7.
4 Molyneux AJ, Birks J, Clarke A, *et al*. The durability of endovascular coiling versus neurosurgical clipping of ruptured cerebral aneurysms: 18 year follow-up of the UK cohort of the International Subarachnoid Aneurysm Trial (ISAT). *Lancet* 2015;385:691–7.
5 Marbacher S, Marjamaa J, Bradacova K, *et al*. Loss of mural cells leads to wall degeneration, aneurysm growth, and eventual rupture in a rat aneurysm model. *Stroke* 2014;45:248–54.
6 Marbacher S, Marjamaa J, Abdelhameed E, *et al*. The Helsinki rat microsurgical sidewall aneurysm model. *J Vis Exp* 2014;92:e51071.
7 Frösen J. Smooth muscle cells and the formation, degeneration, and rupture of saccular intracranial aneurysm wall--a review of current pathophysiological knowledge. *Transl Stroke Res* 2014;5:347–56.
8 Nevzati E, Rey J, Coluccia D. Aneurysm wall cellularity affects healing after coil embolization: assessment in a rat saccular aneurysm model. *J Neurointerv Surg* 2019.
9 Marbacher S, Frösén J, Marjamaa J, *et al*. Intraluminal cell transplantation prevents growth and rupture in a model of rupture-prone saccular aneurysms. *Stroke* 2014;45:3684–90.
10 Gruter BE, Taschler D, Strange F. Testing bioresorbable stent feasibility in a rat aneurysm model. *J Neurointerv Surg* 2019.
11 Grüter BE, Wanderer S, Strange F, *et al*. Patterns of neointima formation after coil or stent treatment in a rat saccular sidewall aneurysm model. *Stroke* 2021;52:1043–52.
12 Frösen J, Marjamaa J, Myllärniemi M, *et al*. Contribution of mural and bone marrow-derived neointimal cells to thrombus organization and wall remodeling in a microsurgical murine saccular aneurysm model. *Neurosurgery* 2006;58:936–44.
13 Fang X, Zhao R, Wang K, *et al*. Bone marrow-derived endothelial progenitor cells are involved in aneurysm repair in rabbits. *J Clin Neurosci* 2012;19:1283–6.
14 Marosfoi M, Langan ET, Strittmatter L, *et al*. In situ tissue engineering: endothelial growth patterns as a function of flow diverter design. *J Neurointerv Surg* 2017;9:994–8.
15 Kilkenny C, Browne W, Cuthill IC, *et al*. Animal research: reporting in vivo experiments: the ARRIVE guidelines. *Br J Pharmacol* 2010;160:1577–9.
16 Nevzati E, Rey J, Coluccia D, *et al*. Biodegradable magnesium stent treatment of saccular aneurysms in a rat model - introduction of the surgical technique. *J Vis Exp* 2017;128.
17 Grüter BE, Täschler D, Rey J, *et al*. Fluorescence video angiography for evaluation of dynamic perfusion status in an aneurysm preclinical experimental setting. *Oper Neurosurg* 2019;17:432–8.
18 Strange F, Sivanrupan S, Gruter BE, *et al*. Fluorescence angiography for evaluation of aneurysm perfusion and parent artery patency in rat and rabbit aneurysm models. *J Vis Exp* 2019;149. doi:10.3791/59782. [Epub ahead of print: 24 07 2019].
19 Kadirvel R, Ding Y-H, Dai D, *et al*. Cellular mechanisms of aneurysm occlusion after treatment with a flow diverter. *Radiology* 2014;270:394–9.
20 Li Z-F, Fang X-G, Yang P-F, *et al*. Endothelial progenitor cells contribute to neointima formation in rabbit elastase-induced aneurysm after flow diverter treatment. *CNS Neurosci Ther* 2013;19:352–7.
21 Raymond J, Sauvageau E, Salazkin I, *et al*. Role of the endothelial lining in persistence of residual lesions and growth of recurrences after endovascular treatment of experimental aneurysms. *Stroke* 2002;33:850–5.
22 Morel S, Karol A, Graf V. Acute pain. *J Neurosurg* 2019:1–14.
23 Marbacher S, Strange F, Frosen J, *et al*. Preclinical extracranial aneurysm models for the study and treatment of brain aneurysms: a systematic review. *J Cereb Blood Flow Metab* 2020;271678X:20908363.